Modelling and measurements of a composite microcantilever beam for chemical sensing applications

I R Voiculescu[1*], M E Zaghloul[2], R A McGill[3], and J F Vignola[3]
[1]Department of Mechanical Engineering, City College of New York, New York, USA
[2]Department of Electrical and Computer Engineering, George Washington University, Washington, USA
[3]Naval Research Laboratory, Washington, USA

The manuscript was received on 11 August 2005 and was accepted after revision for publication on 1 June 2006.

DOI: 10.1243/09544062JMES150

Abstract: A resonant microcantilever beam gas sensor was designed and fabricated in Carnegie Mellon University using complementary metal oxide semiconductor (CMU-CMOS) technology. The cantilever beam modified with a suitable sorbent coating was demonstrated as a chemical transducer for monitoring hazardous vapours and gases at trace concentrations. The design of the cantilever beam included interdigitated fingers to allow electrostatic actuation of the device and a piezoresistive Wheatstone bridge design to read out the deflection signal.The cantilever beam resonant frequency was modelled using the Euler–Bernoulli beam theory and ANSYS. The beam resonant frequency was measured with an optical laser Doppler vibrometer. Good agreement was obtained among the measured, simulated, and modelled resonant frequencies. A custom sorbent polymer layer was coated on the surface of the cantilever beam to allow its operation as a gas-sensing device. The frequency response as a function of exposure to the nerve agent simulant dimethylmethylphosphonate (DMMP) at different concentrations was measured, which allowed a demonstrated detection at a concentration of 20 ppb or 0.1 mg/m^3. The air–polymer partition coefficient K, for DMMP was estimated and compared favourably with the known values for related polymers.

Keywords: cantilever beam, complementary metal oxide semiconductor technology, micro-electromechanical systems, chemical sensing, partition coefficient I

1 INTRODUCTION

A chemical sensor is a transducer that converts chemical information into an analytically useful signal [**1**]. Chemical sensors are important for a variety of industrial, environmental, and military applications, including the detection of hazardous chemicals, quality control in food, perfume, and beverage industries, and medical applications [**2**].

A typical configuration of a chemical sensor includes a sorbent layer deposited on the active area of a transducer [**3**]. The interaction of gas with the sorptive layer is monitored as a function of changes in the physicochemical properties of the sorbent layer and normally transduced into an electrical signal for ease of recording or display.

In this research, the design of the chemical sensor was based on a resonant cantilever beam electrostatically actuated, because of the multiple advantages this sensor has, compared with other chemical sensors. The beam gas sensor is simple to micromachine and to integrate with complementary metal oxide semiconductor (CMOS) technology, with the beam structure created in a post-CMOS fabrication procedure using reactive ion etching. The operating temperature of this gas sensor design is not high, and the frequency stability of the resonator is good.

The microstructure cantilever beam has many interesting applications. Nanoscale cantilever beam

Corresponding author: Department of Mechanical Engineering, City College of New York, 340 West 85th Street, New York, NY 10024, USA. email: ioana@gwu.edu or voicules@ccny.cuny.edu

for biochemical, DNA, and protein sensing has been researched extensively [**4–11**]. Scientists at IBM Research Laboratory, Zurich, Switzerland developed a gas sensor on the basis of a resonant cantilever beam fabricated using CMOS technology, which is magnetically actuated [**12–14**]. Magnetic actuation has a good sensitivity and needs less power, but requires more complex packaging, as a permanent magnet needs to be integrated within the package.

The microstructure cantilever beam was successfully employed in the atomic force microscopy [**15**]. In this case, the cantilever beams with integrated tip and piezoelectric layer for actuation and detection have been microfabricated using monocrystalline silicon as the bulk material.

For designing and modelling a device based on a resonating cantilever beam, a theoretical understanding of its vibration is necessary to estimate the resonant frequency. In this article, the resonant frequency of a composite cantilever beam is computed using the Euler–Bernoulli beam theory. An ANSYS finite-element package and a scanning laser Doppler vibrometer (LDV) were used to simulate and to empirically measure the resonant frequency of the microbeam, respectively.

The fabrication of the cantilever beam gas sensor using CMU-CMOS technology, the Wheatstone bridge arrangement for monitoring the resonance frequency, the electrostatic actuation of the cantilever beam and the experimental details for vapour test measurements have been reported previously, [**16–18**]. The goal of this article is to apply the beam theory to this novel composite cantilever beam fabricated using CMU-CMOS technology. This article also describes the gravimetric application of the cantilever beam gas sensor and offers a modality to calculate the partition coefficient **K**.

2 THE EULER–BERNOULLI LAW OF ELEMENTARY BEAM THEORY

The resonant frequencies of a simple beam with a uniform cross-sectional area and a composite beam are calculated with the assumption that any plane cross-section remains plane during beam bending. The resonant frequency of a thin homogeneous microbeam with a uniform cross-section can be derived by solving the one-dimensional Euler–Bernoulli differential equation (1) [**19–21**]. The Euler–Bernoulli equation models the undamped free transversal vibrations of a cantilever beam

$$\rho A \frac{\mathrm{d}^2 w}{\mathrm{d}t^2} + EI \frac{\partial^4 w}{\partial x^4} = 0 \tag{1}$$

where $w(x,t)$ is the time-dependent transverse displacement of the cantilever beam centre line from the neutral position, EI the bending stiffness, ρ and A the density and the cantilever cross-sectional area, respectively.

This harmonic linear fourth-order differential equation can be solved using separation of variables technique. The displacement $w(x,t)$ can be separated into two parts: one depends on position and another on time, as shown in equation (2). Here, $W(x)$ is the specific shape function, which is independent of time and $Y(t)$ is the time-dependent amplitude, which is independent of position

$$w(x,t) = W(x)Y(t) \tag{2}$$

Substitution of equation (2) into (1) generates two separate ordinary differential equations (3) and (4) [**22**]

$$\ddot{Y}(t) + \omega_{\mathrm{n}}^2 Y(t) = 0 \tag{3}$$

$$\frac{\partial^4}{\partial x^4} W(x) + \omega_{\mathrm{n}}^2 \left(\frac{\rho A}{EI}\right) W(x) = 0 \tag{4}$$

where ω_{n}^2 is a constant equal to the natural frequencies of the microbeam.

Equation (3) is the well-known undamped one-degree-of-freedom harmonic oscillator. The modal shapes for the freely vibrating beam obtained from equation (4) are given in equation (5) [**23**]

$$W_{\mathrm{n}}(x) = \cosh \frac{\lambda_{\mathrm{n}} x}{L} - \cos \frac{\lambda_{\mathrm{n}} x}{L} - C_{\mathrm{n}} \left(\sinh \frac{\lambda_{\mathrm{n}} x}{L} - \sin \frac{\lambda_{\mathrm{n}} x}{L} \right) \tag{5}$$

Here

$$\lambda_{\mathrm{n}}^2 = \omega_{\mathrm{n}} \sqrt{\frac{\rho A}{EI}} \tag{6}$$

where C_{n} are the integration constants, determined by the boundary conditions, and L represents the beam length.

In the case of a cantilever beam clamped at one end, the boundary conditions are $w(0) = 0$ and $w'(0) = 0$ at the fixed end and $w''(L) = 0$ and $w'''(L) = 0$ at the free end of the cantilever. Substituting these conditions into equation (5) yields the frequency equation

$$\cos \lambda_{\mathrm{n}} L \cosh \lambda_{\mathrm{n}} L + 1 = 0 \tag{7}$$

After applying the boundary conditions, the integration constants C_{n} are determined from the

following formula

$$C_n = \frac{\sinh \lambda_n L - \sin \lambda_n L}{\cosh \lambda_n L + \cos \lambda_n L} \quad (8)$$

The roots of equation (7) can be determined numerically. The first three roots are $\lambda_1 L = 1.875$, $\lambda_2 L = 4.694$, and $\lambda_3 L = 7.855$, corresponding to the first three modes of oscillation of cantilever beam.

For the undamped cantilever beam without additional mass, the resonant frequency corresponding to the first mode is obtained using equation (6) and it is equal to

$$f_1 = \frac{\omega}{2\pi} = \frac{1.875^2}{2\pi L^2}\sqrt{\frac{EI}{\rho A}} \quad (9)$$

3 RESONANT FREQUENCY OF A COMPOSITE CANTILEVER BEAM

The cantilever beam fabricated using the CMU-CMOS technology was shown in Fig. 1. The custom style used for the CMOS–MEMS process was developed at Carnegie Mellon University, combined with subsequent micromachining steps [**16**, **24–26**]. The foundry used in this work was Austrian Microsystems (0.6 μm, 3-metal, 2-poly CMOS).

The cantilever beam fabricated using the CMU-CMOS technology is a multi-layer structure fabricated from silicon dioxide, polysilicon, and aluminium thin, layer films which represent standard CMOS layers. The cross-section of this composite microcantilever beam gas sensor was shown in Fig. 2. The natural frequency for the free undamped vibration of a composite cantilever beam can be approximately determined by replacing the bending stiffness EI and density ρ in equation (9) with the composite bending stiffness $\overline{EI}$ and composite

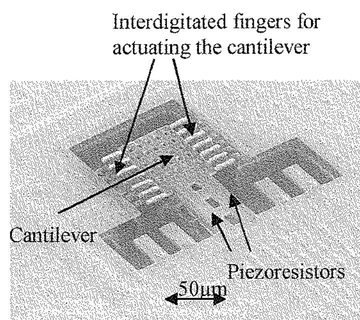

Fig. 1 Micrograph of the cantilever beam

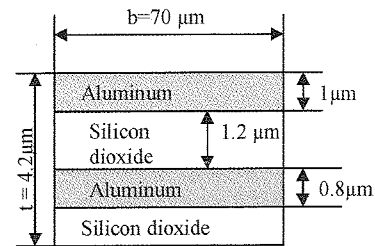

Fig. 2 Cross-section of the cantilever beam shows the combination of CMOS layers

density $\bar{\rho}$ [**27**]

$$\overline{EI} = \sum_{i=1}^{N} E_i I_i \quad (10)$$

$$\bar{\rho} = \frac{\sum_{i=1}^{N} \rho_i t_i}{\sum_{i=1}^{N} t_i} \quad (11)$$

where N is the number of layers in the composite cantilever beam, ρ the density of the individual layers, and t the thickness of the individual layers. Substituting equations (10) and (11) into equation (9) yields equation (12), which is the resonant frequency equation of the composite cantilever

$$f_n = \frac{\lambda_n^2}{2\pi}\sqrt{\frac{\sum_{i=1}^{N} \bar{E}_i \bar{I}_i}{\bar{\rho} A}} \quad (12)$$

where $\lambda_1 = 1.875/L$ corresponds to the wave length of the first mode.

The individual moment of inertia I_i for each layer is computed using equation (13) [**21**]

$$I_i = \frac{bt_i^3}{12} + A_i d_i^2 \quad (13)$$

where b is the beam width, t_i the thickness of an individual film as shown in Fig. 2, A_i the cross-sectional area of an individual layer, and d_i the distance between the centroidal axis of the composite beam and the neutral axis of each individual layer.

The transformed-section method is generally employed to locate the neutral axis of a composite beam [**28**]. The method consists of transforming the cross-section of a composite beam into an equivalent cross-section of an imaginary beam that is composed of only one material. The new cross-section is called the transformed section. The transformed beam is equivalent to the original beam, and its neutral axis is located at the same place as for the original beam.

The principle of the transformed-section method lies in the normalization of each layer with respect to the Young's modulus of the top layer. The width

of each composite layer is given by the following formula

$$b_i = \frac{E_i}{E_N} b \tag{14}$$

where b_i is the width of each normalized layer, E_i the Young's modulus of each layer, and E_N the Young's modulus of the top layer. In this way, the top layer of the transformed beam has the same width b as the original beam, because for the top layer, $E_i = E_N$.

The transformed section of the microcantilever beam cross-section from Fig. 2 is shown in Fig. 3. The mechanically equivalent shape from Fig. 3 has the same Young's modulus as the top layer aluminium. The location d of the neutral plane is found by

$$d = \frac{\sum_{i=1}^{N} d_i A_i}{\sum A_i} \tag{15}$$

where d_i is the distance from the reference layer, which, in this case, is considered the top layer, to the neutral axis of each individual layer. A_i is the cross-sectional area of each individual layer, as shown in Fig. 3.

The resonant frequency of the composite cantilever beam was estimated at 90.812 kHz using equation (12).

4 BEAM VIBRATION SIMULATION WITH ANSYS

For a more accurate study of the composite CMU-CMOS cantilever beam used in this work, finite-element modelling is used to calculate the resonant frequency. The finite-element analysis was performed with ANSYS (version 6.1), and this was used to model the first four resonant frequency modes of the cantilever beam gas sensor, shown in Fig. 4 [**29**, **30**].

The simulations were performed without a sorbent polymer coating. In order to perform the modal

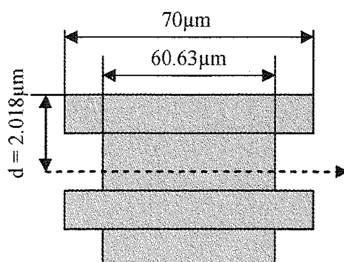

Fig. 3 Transformed cross-section of the same material Al corresponding to the cross-section from Fig. 2. The centroidal axis of the composite beam is marked

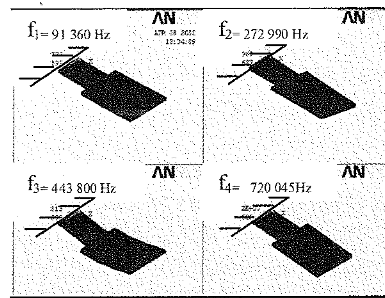

Fig. 4 ANSYS simulation of the cantilever beam resonant frequency. Only the first four modes are represented. The cantilever dimensions are beam length 80 μm, beam width 60 μm, plate length 100 μm, width 70 μm, and thickness 4.2 μm

simulation with ANSYS, the beam was modelled as a composite beam. The mesh elements of the cantilever beam were made using tetrahedral elements (SOLID 92). The material properties of the thin layer used to model the cantilever beam in the ANSYS simulation, such as Young's modulus and density, were given in Table 1 [**14**]. The boundary conditions used for this simulation considered the beam clamped at the left edge, and used at room temperature.

Squeeze-film damping and air-viscous damping were not included in the simulation because the beam has a significant curvature out of the plane and technological perforations, which reduce the effects from air damping.

5 LDV MEASUREMENTS

The surface motion of the microcantilever beam oscillator was characterized with a scanning LDV system developed at the Naval Research Laboratory (NRL). The NRL LDV system has been previously described in detail [**31**]. The system illuminates the sample surface with light from an argon-ion laser (spot size = 2.5 μm). Scattered light for the sample surface is mixed, on the surface of a photodetector, with the frequency-shifted, reference light. The photodetector produces a frequency-modulated signal that, once demodulated, is proportional to the surface displacement at a single location.

Table 1 Material properties of thin layers that form the composite cantilever beam

Material	ν	E (GPa)	ρ (kg/m^3)
SiO_2	0.17	70	2200
Al	0.3	72	2700

The cantilever beam was mechanically vibrated using a piezoactuator, which was driven by a sinusoid that was swept over a frequency range including the fundamental resonant frequency determined from the ANSYS simulation. Figure 5 shows the measured vibration amplitude at the tip of the bare beam, as described in Fig. 1. The frequency corresponding to the maximum amplitude was the resonant frequency and its value was equal to 90.260 kHz.

The cantilever beam, in this work, is normally excited electrostatically by applying an AC voltage superposed on a DC voltage, which results in attractive Coulombic forces between the interdigitated fingers. The beam is set into oscillatory motion in a plane perpendicular to the beam. The circuit used to drive the resonant beam gas sensor has been described previously [**18**]. A spectrum analyser was used to determine the resonant frequency of the device actuated electrostatically. The resonant frequency measured with the LDV system was initially used as the centre point of the frequency range monitored by the spectrum analyser. The resonant frequencies simulated with ANSYS, calculated with equation (12), and measured using the LDV system and electric circuitry are in reasonable agreement and are shown in Table 2. The differences may be partly explained by the absence of a complete simulation, which would include the fingers used for the electrostatic actuation and the etch release holes and also the material properties and thicknesses of the composite layers that were estimated.

6 GRAVIMETRIC APPLICATIONS OF THE MICROBEAM

In this section, the cantilever beam is employed as a picogram microbalance. The principle of operation

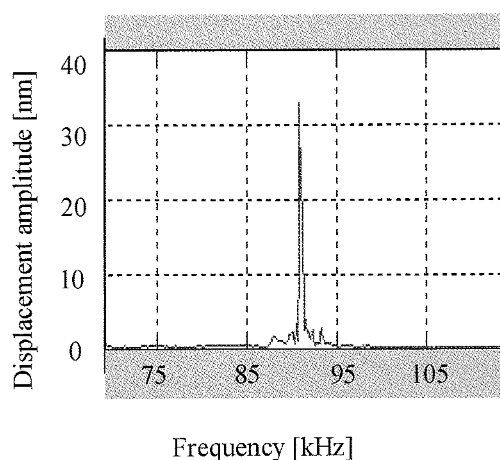

Fig. 5 Vibration amplitude of the cantilever beam as a function of frequency measured with the LDV system

Table 2 Cantilever beam resonant frequency calculated, simulated with ANSYS, and measured with LDV and spectrum analyser

Resonant frequency calculated (kHz)	ANSYS (kHz)	LDV (kHz)	Electrically measured (kHz)
91.812	91.360	90.260	89.900

is based on the mechanical phenomenon that the resonant frequency of a cantilever beam decreases with added mass. The miniature dimensions of the microcantilever beam make its oscillations extremely sensitive to the mass of the gases sorbed to the polymer coating. The amount of mass sorbed to the cantilever beam can be determined from the changes in the resonant frequency of the cantilever. For a uniformly deposited mass, the mass change Δm is estimated using the following equation [**32–35**]

$$\Delta m \approx \frac{k}{\pi^2}\left(\frac{1}{f_1^2}-\frac{1}{f_2^2}\right) \tag{16}$$

where f_2 and f_1 are the resonant frequencies of the cantilever beam before and after absorption, respectively, and k is the spring constant.

In the case of a composite beam, the spring constant is given by

$$k=\frac{3\sum_{i=1}^{N}E_iI_i}{L^3} \tag{17}$$

The spring constant k for a composite cantilever beam from Fig. 1 was calculated as $k = 1.42$ N/m [**33**] and the electrically measured resonant frequency of the cantilever beam was measured as 89.90 kHz. In this work, the polymer was used as a sorbent layer. After the tip of the beam was coated with polymer, the resonant frequency of the cantilever decreased to 88.55 kHz [**18**, **36**]. Using the cantilever beam resonant frequency shift generated by the polymer, the mass of polymer deposited on the cantilever beam was computed using equation (16) as 2.44×10^{-8} g. Assuming the polymer density as 1.6 g/cm^3, the volume of the polymer coat was computed as 1.52×10^{-14} m^3. The cantilever beam gas sensor was tested with different concentrations of dimethylmethylphosphonate (DMMP), which was varied between 0.1 and 43 mg/m^3. The cantilever beam resonant frequency shift as a function of DMMP concentration was shown in Fig. 6. Using equation (16), the mass of analyte sorbed to the polymer layer for different concentrations of DMMP, corresponding to various frequency shifts, was calculated and included in Table 3.

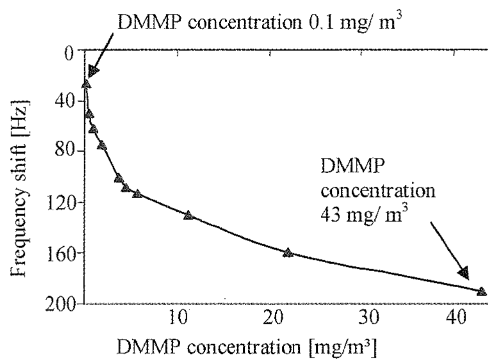

Fig. 6 Beam response upon exposure to DMMP concentrations varying from 0.1 to 43 mg/m^3

7 COMPUTATION OF THE GAS–POLYMER PARTITION COEFFICIENT

The sorption of vapour to a polymer coating is described by the gas–polymer partition coefficient K [**3, 36, 37**]. It is a measure of the strength of the interaction between vapour molecules and the sorbent polymer, where larger K values indicate stronger interactions between the vapour and the polymer. The partition coefficient K is defined (equation (18)) as the ratio between the analyte concentration in the polymer phase, C_p, and the analyte concentration in the gas phase, C_v, at equilibrium, as illustrated in Fig. 7

$$K = \frac{C_p}{C_v} \tag{18}$$

where C_v and C_p can be expressed in mg/m^3.

The log of the partition coefficient for polymers of structure similar to HC, a custom functionalized sorbent carbosilane polymer used in this work, produced at the NRL [**38**], and the analyte DMMP, a simulant for nerve agent, is in the range of 6–9 [**3**].

The polymer coating was produced using only one drop of polymer solution dispensed from an inkjet

Table 3 Mass calculation based on the resonant frequency shift

Δm (10^{-10} g)	Frequency shift, Δf (Hz)	DMMP concentration (mg/m^3)
4.59	25	0.10
7.35	40	0.22
9.18	50	0.50
11.39	62	0.91
13.78	75	1.81
17.46	95	3.63
20.22	110	4.53
23.91	130	5.65
27.59	150	11.23
43.27	235	43

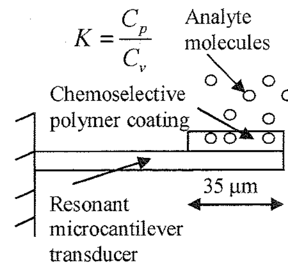

Fig. 7 Polymer-coated microcantilever beam and vapour partitioning coefficient K

head. The inkjet nozzle has an internal diameter of 30 μm; however, the dispensed drop diameter is larger and estimated to be 35 μm. The polymer concentration was 0.03 w/w% in chloroform. Using the cantilever beam resonant frequency shift generated by the polymer, the mass of polymer deposited on the cantilever beam was computed using equation (16) as 5.47×10^{-10} g. Assuming the polymer density as 1.6 g/cm^3, the volume of the polymer coating was computed as 3.42×10^{-19} m^3. The analyte mass, corresponding to a DMMP concentration in the air of 0.1 mg/m^3 and sorbed in the polymer layer, was computed using equation (16) as 4.59×10^{-10} g (Table 3). The partition coefficient characterizing the interaction between the carbosilane polymer and the DMMP was calculated with equation (18), and the log value of the partition coefficient was found to be 8.47, which was in the expected range of 7–9 for similar classes of polymers [**3**].

8 CANTILEVER BEAM MASS SENSITIVITY

The mass sensitivity is calculated in order to compare the microbeam gas sensor with other gravimetric devices. The mass sensitivity is defined as [**39**]

$$S^{\mathrm{m}} = \frac{1}{f}\frac{\Delta f}{\Delta m_{\mathrm{s}}^{\min}} \tag{19}$$

where $m_{\mathrm{s}}^{\min}$ is the minimum detectable surface mass density and it is equal to the minimum detectable mass over an active area of the microcantilever beam.

In the particular case of the microcantilever beam analysed in this article, the minimum detectable mass of 4.59×10^{-10} g is absorbed over an active area of the cantilever beam of 6.89×10^{-6} cm^2. The minimum detectable surface mass $m_{\mathrm{s}}^{\min}$, in this case, is equal to 6.66×10^{-5} g/cm^2. Then, substituting this in equation (19), with $f = 89.90$ kHz and $\Delta f = 25$ Hz, the sensitivity is $S^{\mathrm{m}} = 4.17$ cm^2/g. The DMMP concentration of 0.1 g/m^3 produced a shift of 25 Hz in the resonant frequency. The cantilever beam gas sensor was not tested below this

concentration, so the limit of detection is unknown. If the sensor is working at lower concentrations, the mass sensitivity S^{m} would be expected to be smaller than 4.17 cm^2/g.

The sensitivity of the resonant cantilever beam could also be defined as [**37**, **40**]

$$S = \frac{\Delta f}{C_{v}} \quad (20)$$

where Δf is the frequency change and C_{v} is the analyte concentration in the gas phase. The units are Hz/ppm.

The minimum concentration of DMMP of 0.1 mg/m^3 used to test the gas sensor corresponds to 20 ppb and produces a shift of 25 Hz. The sensitivity S in this case is 1.25 Hz/ppb.

9 DISCUSSION

This article presents the calculation, modelling, and empirical measurements of the resonant frequency of a cantilever beam gas sensor. The values computed for the resonant frequency of the cantilever beam with the Euler–Bernoulli modelling equations and ANSYS simulation agree within 0.5 per cent of each other, with the difference being $\sim$0.5 kHz. However, the empirically determined values were measured at lower frequencies, and for the LDV and spectrum analyser measurements, the resonant frequency agreed within 0.4 per cent of each other. The modelling and empirical measurements offer reasonable agreement and differ by $\sim$2 per cent of each other.

The resonant frequency computation and ANSYS simulation were useful in the process of designing the cantilever beam gas sensor. After the cantilever beam gas sensor was fabricated, the LDV technique was used to determine the actual resonant frequency of the microcantilever beams, because it does not depend on the beam geometry or on the estimate of the material properties. Later, the resonant frequency measured with the LDV system was used as the centre point of the frequency range monitored by the spectrum analyser.

10 CONCLUSION

A composite microcantilever beam fabricated using the CMOS technology was analysed using modelling equations and empirical measurements. The computed values of the resonant frequency and the experimental values were found to be in good agreement. The ANSYS simulation and the Euler–Bernoulli computation were useful in the preliminary microfabrication design process to target a particular resonant frequency and to refine the range examined by the LDV. The LDV technique was used to empirically measure the resonant frequency of microcantilever beams. As a polymer-coated device, the gas–polymer partition coefficient for DMMP was determined with a log value of 8.47, which is in the expected range for the analyte DMMP and the HC polymer used [**3**]. The sensitivity of the gas sensor was also computed.

REFERENCES

1 **McNaught, A. D.** and **Wilkinson, A.** *IUPAC compendium of chemical terminology*, 2nd edition, 1997 (Blackwell Science).

2 **Gardner, J. W., Varadan, V. K.,** and **Awadelkin, O. O.** *Microsensors, MEMS and smart devices*, 2001, Wiley, New York.

3 **McGill, R. A., Abraham, M. H.,** and **Grate, J. W.** Choosing polymer coatings for chemical sensors. CHEMTECH 24, Cedex, France, 1994, pp. 27–37.

4 **Hyun, S.-J., Kim, H.-S., Kim, Y.-J.,** and **Jung, H.-I.** *Mechanical detection of liposomes using piezoresistive cantilever*. Science Direct, 2006.

5 **Villanueva, G., Montserrat, J., Perez-Murano, F., Rius, G.,** and **Bausells, J.** Submicron piezoresistive cantilevers in a CMOS-compatible technology for intermolecular force detection. *Microelectron. Eng.*, 2004, 73–74, 480–486.

6 **Wu, G., Datar, R. H., Hansen, K. M., Thundat, T., Cote, R. J.,** and **Majumdar, A.** Bioassay of prostate-specific antigen (PSA) using microcantilevers. *Nat. Biotechnol.*, 2001, **19**, 856–860.

7 **McKendry, R., Zhang, J., Arntz, Y., Strunz, T., Hegner, M., Lang, H. P., Baller, M. K., Certa, U., Meyer, E., Guentherodt, H.-J.,** and **Gerber, C.** Multiple label-free biodetection and quantitative DNA-binding assays on a nanomechanical cantilever array. *PNAS*, 2002, **99**(15), 9783–9788.

8 **Baselt, D. R., Lee, G. U., Hansen, K. M., Chrisey, L. A.,** and **Colton, R. J.** A high-sensitivity micromachined biosensor. *Proc. IEEE*, 1997, **85**(4), 672–680.

9 **Fritz, J., Baller, M. K., Lang, H. P., Rothuizen, H., Vettiger, P., Meyer, E., Guentherodt, H.-J., Gerber, Ch.,** and **Gimzewski, J. K.** Translating biomolecular recognition into nanomechanics. *Science*, 2000, **288**(5464), 316–318.

10 **Hansen, K. M.** and **Thundat, T.** Microcantilever biosensors. *Sci. Direct Methods*, 2005, **37**, 57–64.

11 **Thaysen, J., Marie, R.,** and **Boisen, A.** Cantilever-based biochemical sensor integrated in a microliquid handling system. Proceedings of 14th Annual International Conference on *Micro electro mechanical systems*, MEMS 2001, Interlaken, Switzerland, 2001, pp. 401–404.

12 **Lange, D., Hagleitner, C.,** and **Brand, O.** *Sensor apparatus with magnetically deflected cantilever*. US Pat. 6 668 627, 1 October 2001.

13 **Vancura, C., Rüegg, M., Li, Y., Lange, D., Hagleitner, C., Brand, O., Hierlemann, A.,** and **Baltes, H.** Magnetically actuated CMOS resonant cantilever gas sensor for volatile organic compounds. IEEE Transducers'03, 12th International Conference on *Solid state sensors, actuators and microsystems*, Boston, 8–12 June 2003, pp. 1355–1358.

14 **Lange, D., Brand, O.,** and **Baltes, H.** *CMOS cantilever sensor systems: atomic force microscopy and gas sensing applications*, 2002 (Springer, Berlin Heidelberg New York).

15 **Indemuehle, P. F., Schuermann, G., Racine, G. A.,** and **de Rooij, N. F.** Atomic force microscopy using cantilevers with integrated tips and piezoelectric layers for actuation and detection. *J. Micromech. Microeng.*, 1997, **7**, 218–220.

16 **Voiculescu, I., Zaghloul, M.,** and **McGill, R. A.** Design, fabrication and modeling of microbeam structures for gas sensor applications in CMOS technology. Proceedings of the 2003 International Symposium, ISCAS '03, Circuits and Systems, Bangkok, Thailand, 25–28 May 2003, vol. 3, pp. 922–925.

17 **Voiculescu, I., Zaghloul, M., McGill, R. A., Houser, E. J., Stepnowski, S., Sokolovski, E., Stepnowski, J., Vignola, J.,** and **Fedder, G. K.** Resonant microcantilever gas sensor fabricated in CMOS technology for the detection of chemical agents. A Solid-State Sensor, Actuator and Microsystems Workshop, Hilton Head 2004, pp. 57–58.

18 **Voiculescu, I., Zaghloul, M., McGill, R. A., Houser, E. J.,** and **Fedder, G. K.** Electrostatically actuated resonant microcantilever beam in CMOS technology for the detection of chemical weapons. *IEEE Sens. J.*, 2005, **5**(4), 641–647.

19 **Shabana, A. A.** *Theory of vibration*, 1991 (Springer-Verlag).

20 **Genta, G.** *Vibration of structures and machines*, 3rd edition, 1998 (Springer-Verlag).

21 **Weaver, W. Jr., Timoshenko, S. P.,** and **Young, D. H.** *Vibration problems in engineering*, 5th edition, 1989 (John Wiley & Sons).

22 **Stark, R. W.** and **Heckl, W. M.** Fourier transformed atomic force microscopy: tapping mode atomic force microscopy beyond the Hookian approximation. *Sur. Sci.*, 2000, **457**(1), 219–228.

23 **Blevis, R. D.** *Formulas for natural frequency and mode shape*, 1979 (Van Nostrand Reinhold Company).

24 **Xie, H., Erdmann, L., Zhu, X., Gabriel, K. J.,** and **Fedder, G. K.** Post-CMOS processing for high-aspect-ratio integrated silicon microstructures. *J. Microelectromech. Syst.*, 2002, **11**, 93–101.

25 **Fedder, G. K., Santhanam, S., Reed, M. L., Eagle, S. C., Guillou, D. F., Lu, M. S.-C.,** and **Carley, L. R.** Laminated high-aspect-ratio microstructures in a conventional CMOS process. *Sens. Actuators*, 1996, **A57**, 103–110.

26 **Guillou, D. F., Santhanam, S.,** and **Carley, L. R.** Laminated, sacrificial-poly MEMS technology in standard CMOS. *Sens. Actuators*, 2000, **A85**, 346–355.

27 **Hossain, N., Ju, J.-W., Warneke, B.,** and **Pister, K. S. J.** Characterization of the Young's modulus of CMOS thin films. Symposium on *Mechanical properties of structural films*, Orlando, Florida, 15–16 November 2000, *STP 1413* (Eds C. Muhlstein and S. B. Brown), (American Society for Testing and Materials, West Conshohocken, PA).

28 **Gere, J. M.** and **Timoshenko, S. P.** *Mechanics of materials*, 4th edition, 1997 (PWS Publishing Company).

29 **Brand, O., Baltes, H.,** and **Baldenweg, U.** Thermally exited silicon oxide beam and bridge resonators in CMOS technology. *IEEE Trans. Electron Devices*, 1993, **40**(10), 1745–1753.

30 www.ansys.com is the website address for the finite element analysis.

31 **Vignola, J. F., Liu, X., Morse, S. F., Houston, B. H., Bucaro, J. A., Marcus, M. H., Photiadis, D. M.,** and **Sekaric, L.** Characterization of silicon micro-oscillators by scanning laser vibrometry. *Rev. Sci. Instrum.*, 2002, **73**(10), 3584.

32 **Thundat, T., Wachter, E. A., Sharp, S. L.,** and **Warmack, R. J.** Detection of mercury vapor using resonating microcantilevers. *Appl. Phys. Lett.*, 1995, **66**(13), 1695–1697.

33 **Yang, J., Ono, T.,** and **Eseshi, M.** Mechanical behavior of ultrathin microcantilever. *Sens. Actuators A, Phys.*, 2000, **82**(1), 102–107.

34 **Lang, H. P., Baller, M. K., Berger, R., Gerber, Ch., Gimzewski, J. K., Battiston, F. M., Fornaro, P., Ramseyer, J. P., Meyer, E.,** and **Güntherodt, H. J.** An artificial nose based on micromechanical cantilever array. *Anal. Chim. Acta*, 1999, 393, 59–65.

35 **Maute, M., Raible, S., Prins, F. E., Kern, D. P., Ulmer, H., Weimar, U.,** and **Goepel, W.** Detection of volatile organic compounds (VOCs) with polymer-coated cantilevers. *Sens. Actuators B, Chem.*, 1999, **B58**(1–3), 505–511.

36 **Houser, E. J., Mlsna, T. E., Nguyen, V. K., Chung, R., Mowery, R. L.,** and **McGill, R. A.,** Rational materials design of sorbent coatings for explosives: applications with chemical sensors. *Talanta*, 2001, **54**(3), 469–485.

37 **Lange, D., Hagleitner, C., Brand, O.,** and **Baltes, H.** CMOS resonant beam gas sensing system with on-chip self excitation. Presented at the 14th IEEE International Conference on *MEMS*, Interlaken, Switzerland, 21–25 January 2001, pp. 547–552.

38 **McGill, R. A.** and **Houser, E. J.** *Linear chemoselective carbosilane polymers and methods for use in analytical and purification applications*. US Patent 6 660 230.

39 **Datskos, P. G.** and **Sauers, I.** Detection of 2-mercaptoethanol using gold-coated micromachined cantilevers. *Sens. Actuators B*, 1999, **61**, 75–82.

40 **Lange, D., Koll, A., Brand, O.,** and **Baltes, H.** CMOS chemical microsensors based on resonant cantilever beams. Conference on *Smart electronics and MEMS*, SPIE, San Diego, 1998, vol. 3328, pp. 233–243.